THIRD QUARTER 2006 www.sme.org/pcc VOL. 5, NO. 3

Latest-Generation SLA Resins Enable Direct Tooling for Injection Molding

Alexander K. Do, Paul K. Wright and **Carlo H. Sequin,**
University of California, Berkeley

The set of fabrication processes classified as rapid prototyping (RP) technologies have shown to be effective low-cost tools for prototyping parts, primarily in areas of design validation. Generally, RP refers to any process that uses a layer-based solid freeform fabrication method to create physical parts directly from digital CAD data. Prototypes and models built from RP have been used for interaction between disciplines in product development: design, engineering, marketing, buyers and manufacturing. However, material properties, quality factors, costs and lead times of RP processes have limited their viability as methods of direct production.

In recent years, RP has been used in direct and indirect methods to fabricate injection mold tools, with varying results. Examples of such work include research by Dickens and Smith [1] and Harris et al. [2-4]. The ability to fabricate injection molding tools directly from RP would dramatically simplify production of injection-molded parts. However, the processes for doing so are still in their infancy, and there is a lack of extensive knowledge and literature about them. In this research, a low-cost injection mold tool was directly fabricated from high-resolution stereolithography with a composite resin and evaluated for viability as a short-run tooling option.

Review

Direct and Indirect Tooling Methods. An indirect RP tooling method refers to a process in which a rapid-prototyped master part is used as a casting pattern for a final molding tool. One example of indirect tooling is the spray metal tooling method [5] in which an RP model is sprayed with fine droplets of molten metal, creating a metal shell about 0.08 in. (0.2032 cm) thick. The shell is backed with an epoxy filling, allowing for the integration of cooling channels and an ejection system. Another casting method that uses a sintered metal-powder mixture is the 3D Keltool process [6]. The 3D Keltool process can be used to produce a cavity and core set or to build an electrical discharge machining (EDM) electrode for creating hard metal tooling. Indirect methods have been proven with accurate and durable tools, but the availability of processors is limited; for example, the 3D Keltool process requires an operating license, and a considerable amount of post-processing of tooling parts could be required.

Direct tooling methods, by contrast, use RP technologies to produce the final mold core and cavity. In addition to Dickens' work in stereolithography [1], other processes such as Z-Corp.'s 3-D printing have been studied in injection molding [7]. While direct tooling methods offer the ability to easily produce a tool in-house or through a service bureau, the limiting factors in material properties have prevented them from becoming industry standards for short-run injection molding.

Composite SL Resins. Stereolithography (SL) resins have long been studied for direct injection mold tooling, but material and process limitations in accuracy, durability and heat resistance hindered practical applications [8]. Previous work has generally indicated three challenges of direct SL tooling: susceptibility of core to failure during injection and ejection, possibility of instantaneous failure through fracture and unforeseen effects of thermal properties [2-4]. Composite resins recently introduced by materials manufacturers DSM Somos and 3D Systems offer dramatically increased performance in material properties and could potentially address early challenges in direct SL tooling. The materials employ a matrix of thermosetting polymer (usually acrylate and/or epoxy resins) around a reinforcing type of ceramic, which is used to provide stiffness, strength and heat resistance while maintaining the manufacturability of stereolithography. The reinforcing ceramics used have typically been silica, with particle sizes ranging from 10-999 nm for “nanoparticles” and 1-100 µm for “microparticles.” The composite materials available at the time of this writing consist of ProtoTool and NanoForm by DSM Somos [9] and Accura Bluestone by 3D Systems [10]. The properties for these materials, listed in *Table 1*, show similar levels of increased strength and heat deflection temperatures over unfilled resins. The materials do, however, differ in modulus, glass transition temperature (T_g) and coefficient of thermal expansion (CTE).

Property	Accura Bluestone	DSM Somos ProtoTool 20L	DSM Somos NanoForm 15120
Tensile strength	9.6-9.8 ksi	10.4-11.4 ksi	7.7 ksi
Modulus of elasticity	1,100-1,700 ksi	1,465-1,624 ksi	856 ksi
Flexural strength	18-22.3 ksi	17.1-17.8 ksi	18.7 ksi
Flexural modulus	1,200-1,417 ksi	1,340-1,392 ksi	645 ksi
Compressive strength	*no data	22.2 ksi	34 ksi
Compressive modulus	*no data	1,470 ksi	678 ksi
CTE 32°F to 302°F (–17°C to 150°C)	18-54 x 10^{-6} in/in-°F	21-51 x 10^{-6} in/in-°F	28-71 x 10^{-6} in/in-°F
T_g	160°F to 181°F (71°C to 83°C)	120°F (49°C)	176°F (80°C)
HDT @ 66 psi	513°F to 543°F (267°C to 284°C)	495°F to 498°F (257°C to 259°C)	517°F (269°C)
HDT @ 264 psi	*no data	181°F to 201°F (83°C to 94°C)	240°F (116°C)

***Table 1.** Material properties for composite SL resins [9,10].*

Of the three composite materials, NanoForm was chosen for this study for its ability to form small features accurately. While NanoForm offers lower tensile strength than ProtoTool or Bluestone, it is the only composite resin that can currently be run at high-resolution build mode on an SLA Viper. The high-resolution build mode enables a 0.002 in. (0.0051 cm) layer thickness and 0.003 in. (0.0076 cm) beam diameter – contrasted to 0.004 in. (0.0102 cm) layer thickness and 0.010 in. (0.0254 cm) beam diameter in standard build modes [11,12]. This was particularly advantageous for the study because of the geometric features intended for the mold, which included sharp corners and pronounced angular features. In addition, the material is the least brittle of the group, a characteristic that could be beneficial to tool life. Another unique NanoForm property is that the nanoparticles maintain their suspension in the uncured resin without vat mixing or stirring, unlike ProtoTool or Bluestone.

SLA Direct Tooling Molding Process

The total design and manufacturing process used for the short-run injection molding study is similar to the process that would be taken for a standard production-quantity mold:

1. Design and validate part:
    - Design for manufacturability (DFM) analysis
    - Rapid prototyping
2. Design mold and ejection system:
    - Cavity scaling factor
    - Parting line
    - Runners, gating, venting
3. Partition cavity/core features to mold inserts:
    - Mechanism to secure inserts
    - Mold cooling design
4. Fabricate SL inserts and mold base:
    - Outside service bureau or in-house
5. Determine injection parameters by testing:
    - Injection pressure and speed
    - Clamping force
    - Holding and cooling time

The primary novelty in this process occurs during Step 3, the partitioning of cavity and core features to SL inserts. Generally, cavity and core features are formed by a single or multiple metal parts in a production tool, which are pressed or bolted into the mold assembly. Similarly, designing a mold assembly to use SL cavity and core inserts, which can be secured into a metal base, allow the complex geometric features to be rapidly manufactured by SLA. Securing these inserts into a base rather than fabricating the entire tool from stereolithography allows for a number of benefits:

- Reduced amount of volume to be built on SLA, reducing lead time and cost.
- Use of a generic mold base for a family of interchangeable SL inserts, reducing tool costs.
- Installation and mating of the assembly to standard platen / nozzle interfaces, which create better distribution of clamping force through the hard-metal mold base.
- Simpler installation of alignment, ejection and cooling systems.
- In the case that the tool fails or needs considerable adjustment in geometry, a new insert can be fabricated quickly at a low cost.

Fabrication of the SL inserts can be done in-house with SLA equipment, but with the widely available number of service bureaus, it can be very simple to use a third-party vendor for this process. Some service bureaus, such as Quickparts.com, offer electronic online quoting systems, and many other vendors will accept files by e-mail and return quotes within hours. This enables a particularly good lead time for fabricating the inserts, typically as fast as one week, including shipping.

The process, assuming access to a molding press and a stock of molding materials, can cost anywhere from $1,000 to $6,000 or more depending on size, complexity and materials. A summary of the approximate costs and turn time:

- Aluminum mold base: $500-$3,000 depending on material, machining time, in-house capabilities
- SL inserts: $500-$3,000 depending on material, volume, *z*-height (build time), layer thickness
- Alignment and ejection hardware: $100
- Turn time: One to two weeks

Design of Mold Cavity Set

Part Geometry. The part intended to be molded from the tool was a flat tile, roughly 0.125 in. (0.318 cm) thick at the edges and 0.0625 in. (0.1588 cm) thick in the center, with a projected surface area of roughly 3.5 in^2 (8.9 cm^2). The CAD rendering for the tile is pictured in *Figure 1*. In particular, these tiles had unique features, which would be difficult to machine into a mold: sharp angles, well-defined teeth and two parting planes. The tiles were designed to form larger building blocks by mating with each other at the teeth, so part accuracy was important to maintain.

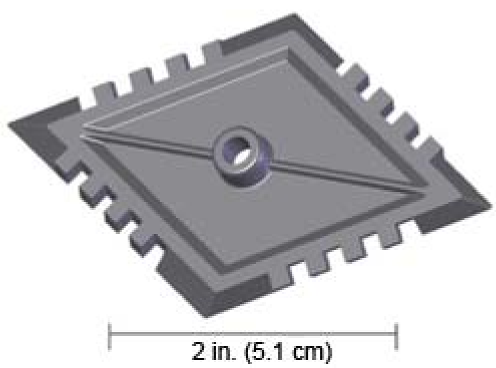

Figure 1. *CAD rendering of zonohedra tile.*

Cavity and Core Inserts. The mold assembly consisted of aluminum blocks for alignment and distribution of clamping force, SL cavity and core inserts secured by flange screws, two hardened steel locating pins and two hardened steel ejector pins. No active cooling was designed into the mold assembly – instead the mold would need to be air-cooled between shots. The cavity and core inserts for the mold assembly were designed to minimize volume and thickness so that the cost of the SL inserts would be minimal. The *x* and *y*-dimensions of the cavity and core inserts were 6 x 4 in. (15.24 x 10.2 cm), and the *z*-dimensions were 0.4 and 0.25 in. (1.02 and 0.64 cm), respectively. The aluminum base parts, made from 6061-T6 for ease of machining, measured 8 x 6 x ~1.25 in. (20.32 x ~3.18 cm). The pockets in the aluminum base were also designed with 0.015 in. (0.0381 cm) of relief over the length and width dimensions of the inserts, so that any thermal expansion of the inserts would be unbounded. The locating pins were pressed into the aluminum blocks to align the cavity and core. The mold was designed for manual loading, opening and ejection on a Morgan Press GT100.

The inserts were fabricated by Protogenic Inc. with Somos NanoForm 15120 on an SLA® Viper in a high-resolution build. Except for basic support removal and UV/thermal post-curing, no added post-processing, such as polishing or finishing inside diameters of holes, was performed on the inserts so that issues resulting from the SLA process could be analyzed. *Figure 2* shows the mold assembly for the cavity and core.

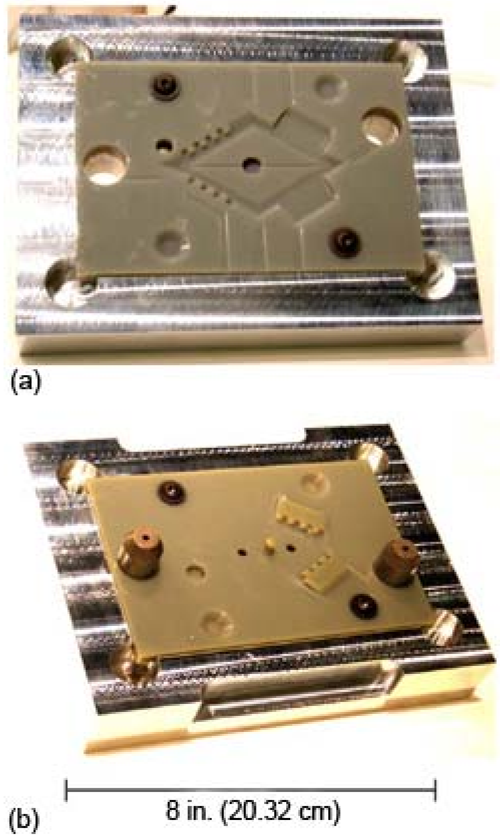

Figure 2. *Mold top with cavity insert (a), mold bottom with core insert and locating pins (b).*

Molding Experiment

The mold cavity and core were tested on a Morgan Press GT100, a small 20 ton manual injection molding press, to evaluate tool quality, part quality and process repeatability. The blend of ABS used was a standard unfilled material, Lustran 648. Once the optimal injection molding parameters were determined, the tool was tested until it was used for 150 total shots.

The injection molding parameters for the tool were determined by beginning at minimal energy parameters (low temperatures, clamping force, injection speed and injection pressure) to protect the tool and adjusting these parameters based on part quality indications. The first set of parameters used was: 450°F (232°C) barrel and nozzle temperature, 12 tons of clamp force and 6,000 psi injection pressure. Because the Morgan Press uses a pneumatic ram to force injection, it does not have control over the actual flow rate. Instead, the ram adjustment is made with a unitless setting on an orifice, which controls the pneumatic airflow to the ram. The tool was loaded into the press and preheated before steady-state molding with a heating plate, and it was found that during steady-state the heating plate needed to be turned off, otherwise the core and cavity temperatures would remain too high for quality parts. Silicone mold-release spray was used sparingly every few shots to aid in part ejection. The gate was mistakenly designed too small at 0.032 in. (0.0813 cm) thick by 0.28 in. (0.7112 cm) and based on molding results was expanded by about 0.015 in. (0.038 cm) by filing material away from the core insert.

During the initial molding trials, the mold was tested under a wide range of injection parameters, as shown in *Table 2*:

Barrel temperature	450°F to 470°F (232°C to 243°C)
Nozzle temperature	450°F to 477°F (232°C to 247°C)
Clamping force	12-16 tons
Injection pressure	6,000-9,000 psi
Ram speed	Med-high – high
Shot and hold time	2-25 sec.
Preheat	0°F to 140°F (–17°C to 60°C)

Table 2. *Operating range of mold in experiment.*

After a large number of shots, the ideal operating conditions for the mold were determined, as outlined in *Table 3*:

Barrel temperature	465°F to 470°F (241°C to 243°C)
Nozzle temperature	Barrel temp. + 5°F (–15°C)
Clamping force	16 tons (maximum attainable)
Injection pressure	7,000 psi
Ram speed	High
Shot time	2.5 – 3 sec.
Preheat	None during steady-state, 140°F (60°C) to bring up cold mold to temperature

Table 3. *Injection molding parameters used.*

The temperature and pressure parameters are at the lower end of the plastic manufacturer's recommendation, while the mold temperature and injection speed are comparable to the recommended levels. Once the optimal parameters were determined, the tool was tested until it was used for 150 total shots. Each part was batched by parameter grouping and evaluated to determine quality.

A somewhat steady-state cycle was achieved in spite of variations in flash and sink – hindered slightly by both the timing of manual operations (such as injection control and clamp operation) and thermal control of the mold assembly. The ideal shot time was somewhere between 2 and 3 sec., with too short of a time causing short shots and too long of a time causing potentially large amounts of flash. The approximate cycle times attained under the optimal molding conditions (*Table 3*) are presented in *Table 4*:

Injection and packing	2.5 sec., ± .5 sec.

Holding (no packing pressure)	10 sec.
Part cooling in mold	45 sec.
Mold opening and ejection	20 to 30 sec.
Mold cooling and hopper refill	20 to 30 sec.
Alignment and clamping	10 to 15 sec.
TOTAL	2 min.

Table 4. *Cycle time under steady-state.*

Results and Discussion

Overall, the results of the experiment were encouraging; despite a minor core feature that fractured on the first shot, the tool was used over 150 times and produced parts with exceptional definition. The tool did exhibit some wear, but it was minimal. The gate (which was mistakenly designed much too small) began to suffer from minor chipping after about 50 shots, and two hairline fractures appeared nearly 100 shots into the process, but these problems did not detract from the overall part quality. Accuracy of the part was very repeatable, with parts showing no warp and consistent size. Repeatability in aesthetic part quality was fairly difficult to attain, however, and was not achieved to satisfaction. The variability in flash was fairly high, and the nature of the sink tended to vary a bit from part to part. It is believed that the primary challenge to repeatability was the poor control of process parameters on the molding press used. The clamp force could not be increased to control flash because the press was at its maximum level, the injection timer on the machine was nonfunctional and the machine had no designed control of shot weight or volume. An interesting observation from the experiment is that the parts consistently ejected better when their temperature was below the inserts glass transition temperature (T_g), 176°F (80°C). During one trial in which the mold was opened rather quickly, the temperature of the part at the center (0.0625 in. [0.1588 cm] wall thickness) was approximately 180°F (82°C), while the temperature at one of the teeth sections (0.125 in. [0.318 cm] wall thickness) was over 200°F (93°C). The temperature of the SL mold at that particular tooth block was measured at 190°F (88°C), more than 10° above its T_g. Under these conditions, ejection was quite difficult as the part would bend up with the ejection pin while the teeth on the part stuck to the blocks on the core.

The ensuing results and discussion of this article are focused on three key unique issues discovered during the experiment: the dimensional accuracy of NanoForm in high-resolution build mode, geometric design issues in the mold core and thermal management of the tool.

Dimensional Accuracy. An unexpected issue with the tool was that serious anisotropy in dimensional accuracy of the inserts was revealed when the tool fractured during the first assembly. The inserts were fit into the aluminum bases and appeared to fit well enough (they were very snug on the locating pins) until the entire mold assembly was closed together to see how well it fit. The closure between the cavity and core was very snug at the two sliding shutoff areas where the parting line jumps from one plane to another. Upon opening the mold, the core insert fractured instantly, with an entire tooth block breaking off of the core. The fracture and tooth block are shown in *Figure 3*.

Figure 3. *Core insert showing brittle fracture (a), tooth block after separation from core (b).*

Following the fracture, it was suspected that the core and cavity inserts were not within the original design tolerance, so they were measured with calipers. The width of the cavity gaps, which interfaced with the tooth blocks from the core, were 0.002 in. (0.0051 cm) smaller than the original dimensions, while the block that fractured was 0.003 in. (0.008 cm) wider at the base than designed. In total, 24 cavity parameters and 17 core parameters were measured. Two parameters, which were offset by a relatively significant amount, coming from approximately 0.010 in. (0.0254 cm) overshoot of the plate thicknesses of both inserts, were later excluded from analysis because the vendor stated they would not be within specification without post-processing (as a result of the necessary support base during the SLA process). The offsets from the design specifications of the remaining 39 measurements ranged from +0.005 to –0.027 in. (+0.013 to –0.0686 cm), with a mean value of –0.004 in. (–0.0102 cm) and a standard deviation of 0.006 in. (0.01524 cm).

A histogram of offset errors is presented in *Table 5*. The histogram shows the majority of the offsets fall within the bin for 0, –0.005 in. (0, –0.013 cm). The table also shows a strong weighting toward negative offset errors, corroborating the mean value of –0.004 in. (–0.01012 cm). From these two parts, the resultant natural tolerance (following the ± 3s model) of NanoForm in this particular high-resolution build from the SLA Viper is determined as (+0.014 in. [+0.0356 cm], –0.022 in. [–0.0588 cm]).

Bin	Frequency
–0.030 in. (0.076 cm)	0
–0.025 in. (0.064 cm)	1
–0.020 in. (0.051 cm)	1
–0.015 in. (0.038 cm)	0
–0.010 in. (0.0254 cm)	2
–0.005 in. (0.013 cm)	8
0 in. (0 cm)	21
+0.005 in. (0.013 cm)	6
> +0.005 in. (0.013 cm)	0

Table 5. *Histogram data for cavity and core offset errors.*

Because there was a limit to measurement accuracy with calipers for many of the dimensions, as well as a process capability limitation outlined by the vendor (±0.005 in. [0.013 cm]), all offsets which were greater in magnitude than 0.005 in. (0.013 cm) were compared. What was found was that of these 12 larger offsets, 11 of the errors were from “female” type features, consisting of inside diameters of holes or widths of cavity/gap features. The other types of features that were characterized were “male” features consisting of diameters and widths of protruding material, and “depth” features, which were dimensioned along the layer axis (*z*-axis).

Characterization of the 39 dimension parameters showed the following trends:

- female features smaller than designed (all); mean offset –0.008 in. (–0.02032 cm), standard deviation of 0.006 in. (0.01524 cm)
- male features very accurate (most); mean offset –0.001 in. (–0.00254 cm), standard deviation of 0.004 in. (0.0102 cm)
- depth features within 0.002 in. (0.0051 cm) layer resolution
- hole centers on target (*x*-*y* location)

The resulting anisotropy in accuracy can be identified as the cause of the initial tooth block fracture; the slightly larger block was press fit into the smaller cavity. It is not believed that this error could be accounted for beforehand in the design, as sliding shutoffs in molds require a very narrow tolerance. The offset errors of the female features were inconsistently deviant from the original design parameters; they were offset by neither an absolute amount nor linear ratio. The offset magnitudes ranged from 0.002 to 0.013 in. (0.0051 to 0.03302 cm) and the percent error from 0.2% to 5%. As a result, a mold designer would be unable to compensate for this in a CAD model.

Conversations with an industry operator confirmed that they had seen a similar issue in dimensional accuracy, though no publications on the matter are known to exist at the time of this writing. It is not known whether the problems in accuracy were a result of configuration of the SLA machine used to build the part, but that is not believed to be the case because the accuracy of male features was within expectation and considerably better than that of female features. At the time of this writing, interviews with three SLA processors revealed that there has not been much industry experience with the NanoForm material built in high resolution. More investigation into the interaction between material properties and process control are necessary to determine the cause of the anisotropy. In particular, the algorithms used to trace the laser path for polymerization initiation should be studied against the material chemistry and geometric modeling engines. The problem likely stems from the fact that female features are bounded by bulk resin material, which shrinks as a result of cross-linking—during both initial curing and continued post-curing; therefore, implying a nonlinear geometric transformation to final part geometry.

Tool Geometry. A number of lessons were learned about considerations for tool geometry when using this tooling process. The primary lesson is in the design of certain core features when a certain heigth-width ratio is exceeded. The first injection produced an encouraging result, as shown in *Figure 4*. However, not enough care was taken during mold opening to ensure that the sprue remained on the core side, causing the part to bend upward with the cavity (anchored to the sprue by the gate), which in turn immediately sheared the core pin from the core insert. While a small fillet was designed in to reduce stress concentration, the pin broke just above the fillet. The pin broke nearly straight across, but managed to gouge one or two layers below into a small bowl-like shape on the core and a corresponding flat dome-like shape on the fractured pin. Molding was continued with the absence of this feature to continue testing the tool. It was not believed that the pin would have remained set if bonded back to the core, due to the perpendicular orientation to rapidly flowing viscous plastic during injection. The pin diameter was 0.1875 in. (0.4763 cm) and the pin height was 0.28 in. (0.7112 cm), giving an aspect ratio of nearly 1.5. While recommended aspect ratios have not yet been quantified for this material, this type of feature is probably best fabricated with a metal insert.

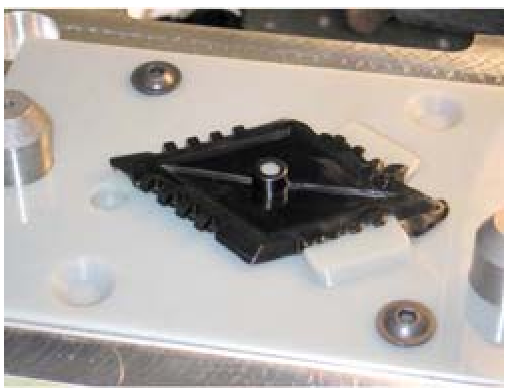

Figure 4. *Shot 1 in mold (sprue removed for picture).*

The gate, as stated earlier, was mistakenly designed at a thickness of 0.032 in. (0.0813 cm) for a part that had a primary wall thickness of 0.0625 in. (0.1588 cm) and a perimeter thickness of 0.125 in. (0.318 cm). Expanding the gate by 0.015 in. (0.0381cm) with a small file noticeably relaxed sensitivity of part quality to changes in molding parameters, though the process would have likely benefited from a gate closer to twice its original size (0.65 in. [1.651 cm]). Before the gate was expanded, the parts were more susceptible to blemishes and ripple lines. It is recommended that as large a gate as possible is used, especially because of the thermal properties which are discussed in the following section.

The errors in plate thickness, which were excluded from previous analysis, can have an effect on the mold construction as well, as they affect hybridization with other components, such as the ejection system and any metal inserts secured to the base. For example, the ejector pins are mounted onto an ejector plate from below, which must be aligned such that the pins are flush with the surface of the core; any variations in the core thickness will require adjustment of the ejection system. It is therefore recommended to request finishing of the insert bases from the service bureau or to finish them independently with a milling machine.

Thermal Management. The unique thermal properties of the mold inserts affected cycle times, part quality, repeatability and possibly tool life. One observation of unique thermal properties was the occurrence of two small cracks believed to be a result of thermal stresses. After 50 shots, a small hairline crack was discovered in the core of the mold, seen in *Figure 5a*. The crack measured about 0.21 in. (0.5334 cm) and extended from the corner of the base of the repaired tooth block along the approximate outline of the cavity parting line. The crack was very difficult to see in most lighting conditions and there was no noticeable gap. Another similar hairline crack was discovered after 90 shots in the cavity, pictured in *Figure 5b*. This crack was considerably larger, measuring nearly 0.84 in. (2.134 cm) long. The crack ran from a corner of the parting line vent down to the part top (base layer of the cavity), along the edge of the cavity wall and into the shutoff area where the cavity meets a tooth block from the core. It is not known when the cracks first developed, as they are inconspicuous under most lighting conditions. Once they were discovered, neither crack seemed to propagate with continued cycling for the rest of the experiment, and there was no perceived effect on part quality.

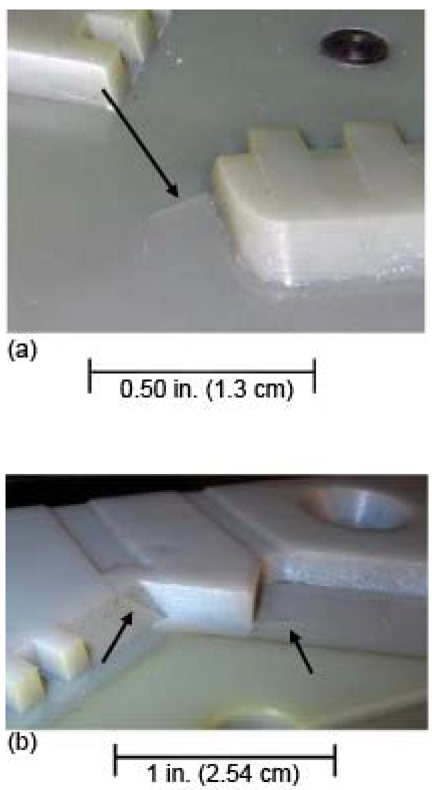

Figure 5. *Hairline cracks in core (a) and cavity (b).*

It is believed that the cracks were initiated to relieve internal stresses occurring during the injection and cooling cycles. Considering that the cooling rate was uneven within the mold, the thermal conductivity of the material is low and the coefficient of thermal expansion is appreciable, resulting stresses could easily account for the fractures pictured in *Figure 5*.

While fully constrained thermal expansion would cause compressive stresses which would not lead to crack propagation, differences in cooling rate would create tensile stresses leading to crack growth. Both of the cracks initiated from stress concentration points and traced along the outline between cavity and shutoff area; the cooling rate of the inserts at an interface with the molded part would be expected to be slower than at the shutoff.

A study of the temperature distribution of the mold revealed that the temperatures were quite variable spatially and temporally throughout an injection and cooling cycle. From measuring the mold temperatures with an infrared thermometer during different part cooling and mold cooling times, it was found that the amplitude of a thermal cycle for a given mold section was generally at least 60°F (16 °C) in areas which contacted the ABS plastic. Specifically, the temperature of the repaired tooth block typically went from 120°F (49°C) to at least 190°F (88°C) during the injection cycle. Without an instrument to continuously monitor the temperature through the molding cycle, the peak temperatures could not be determined, so instead, the mold was opened with minimal cooling time in some instances to record the temperatures of the hotter areas. *Figure 6* shows a thermal map of the mold temperatures after part ejection, with each measurement taken immediately after part ejection under steady-state molding. The map shows a high spatial variation of temperatures in the mold, with as much as 60° difference between molding areas and shutoff on the inserts. It should be noted that during the peak of the molding cycle, this difference was likely closer to the order of 100° F (38°C).

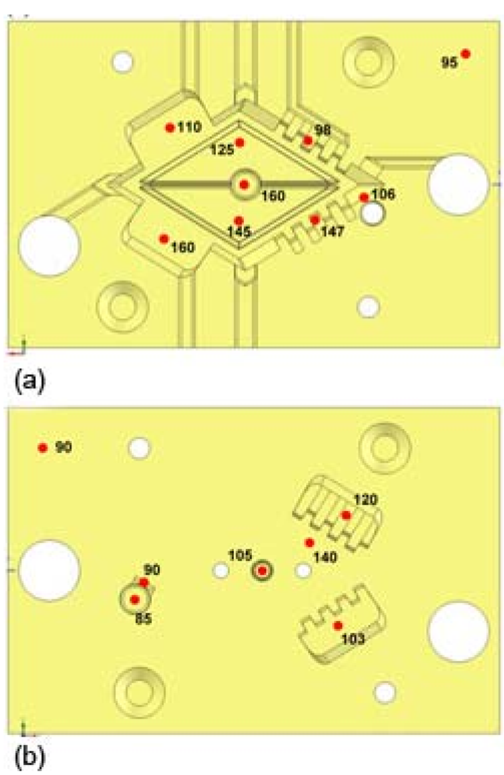

Figure 6. *Typical mold temperature distribution after part ejection in cavity (a) and core (b) (°F).*

Minor variations in sink from part-to-part, while exacerbated by a small gate and poor control of shot timing were likely also a partial result of the difficult control of mold temperature. For example, it was found that when the barrel and nozzle temperatures were increased to lower resin viscosity, the parts began to show dramatically more sink in the thicker areas – demonstrating uneven cooling. The levels of sink experienced were acceptable in an early prototyping process, but were unacceptable if high-quality parts comparable to those from production injection molding are desired.

As mentioned earlier, the low thermal conductivity of NanoForm contributed to cycle times, which were much longer than what could be expected from a metal tool. The thermal conductivity of NanoForm is 0.09 lbs./s-°F (0.7 W/m-K) , compared to that of aluminum: 25 lbs./s-°F (200 W/m-K)—the ratio between the two is greater than 275. An active cooling system may reduce the cycle time and possibly enhance repeatability, but could also introduce more stresses into the tool that would affect its life. Ultimately, finite element analysis of the tool is necessary to understand whether active cooling and/or heating would improve or degrade the tool life.

Conclusion

In this study, 150 parts were injection molded from ABS with a tool built from NanoForm 15120 in high-resolution. The cost of the tool was less than $2,500 and the total lead time was less than three weeks, including molding time and costs, favorably comparing it to accepted rapid tooling alternatives. Although only one of the parts was completely “usable” as molded (because all others lacked a through-hole), a large number were post-processed and used to study design changes for a second round. The parts showed good accuracy, strength, definition of features, but also contained aesthetic flaws. It should be noted that despite the increased material performance and competitive costs, the early challenges of direct tooling with SL, while ameliorated, are still issues potential users should be aware of. NanoForm tooling can undergo instantaneous failure from brittle crack propagation and/or delamination, especially at stress concentration points, and the thermal properties of the cured resins pose challenges to injection molding. Despite the learning curve and challenges, it is concluded that injection mold tooling made with composite SL resins is viable for use in short-run injection molding, allowing for the production of hundreds of parts. It is believed that with fine control of process parameters, the process repeatability will be acceptable for a majority of small-to-medium-sized parts (1 to 5 in. [2.54 to 12.7 cm] cross section).

Lessons Learned. A number of general tool design and process lessons were learned in this study. They are summarized here as general rules that can aid the effectiveness of future projects:

- Avoid or minimize stress concentrations in tool design.
- Depending on aspect ratio, some parts of core should be made as metal inserts.
- Sliding shutoffs very difficult in SL because the accuracy is still not good enough without post-processing.
- QC and post-processing of SL inserts a good idea for high-accuracy molds (better than ±0.02 in. [±0.051 cm] accuracy).
- Make a big gate to counteract thermal properties of core and cavity.
- Ejection easier once mold is below T_g.
- Use injection molding equipment with fine control of process parameters.

Further Research. Two areas beckon continued research: (1) the thermal management of SL tooling and dimensional accuracy of the cavity and core—to address the thermal issues, comparison of tool life and part quality should be studied under use of different cooling strategies; and (2) the SLA community (developers and researchers of software, equipment and material, and also service providers) is urged to jointly investigate the problem of anisotropy in dimensional accuracy in the hope of continuing to push the envelope on direct tooling capabilities.

Acknowledgments

For their contributions to this research, the authors wish to acknowledge the following individuals and corporations:

- Dan Odell, UC Berkeley
- Xiaorui Chen, UC Berkeley
- Lisa Pruitt, UC Berkeley
- Tim Nakari and Jason Boh, Protogenic
- Paul and Bret Bordner, Laser Reproductions
- Brian Bauman, DSM Somos
- Mike Daniels, Production Robotics
- Erik Appelbom, Jatco
- Tom Hagen, Poly-Tek

Funding and research facilities were made available by Ford Motor Co., CITRIS and by the California Energy Commission under Grant Award DR-03-01.

References

[1] Dickens, P.M. and Smith, P. "Stereolithography Tooling." *Proc.* of 1st European Conf. on Rapid Prototyping, 1992, pp309-317.

[2] Harris, R.A.; Newlyn, H.A.; Hague, R.J.M.; and Dickens, P.M. "Part Shrinkage Anomalies from Stereolithography Injection Mould Tooling." *Int'l Journal of Machine Tools & Manufacture* (v43, 2003), pp879-887.

[3] Harris, R.A.; Newlyn, H.A.; and Dickens, P.M. "Selection of Mould Design Variables in Direct Stereolithography Injection Mould Tooling." *Proc.* of the Institution of Mechanical Engineers, Part B, *Journal of Engg. Manufacture* (v216, nB4, 2002), pp499-505.

[4] Harris, R.; Hopkinson, N.; Newlyn, H.; Hague, R.; and Dickens, P. "Layer Thickness and Draft Angle Selection for Stereolithography Injection Mould Tooling." *Int'l Journal of Production Research* (v40, n3, 2002), pp719-729.

[5] Martyniak, S.A. "Prototype and Limited Production, Spray Metal Tools for Injection and Blow Molding." *Proc.* of SME's Rapid Prototyping and Manufacturing Conf., 1993.

[6] Gebhardt, A. "Rapid Prototyping." Cincinatti: Hanser Gardner Publications, 2003.

[7] Hackney, P.M. and Pancholi, K.P. "Analysis of the Application of the Z-Corps Three-Dimensional Printing System for Rapid Tooling for Plastic Injection Moulded Components." 5th Nat'l Conf. on Rapid Design, Prototyping, and Manufacturing, Lancaster Univ., Lancaster, England, 2004.

[8] Williams, J. and Kaufmann, C. "Injection Molding with Composite Stereolithography Resins." RAPID 2005, Dearborn, Mich.: Society of Mfg. Engineers.

[9] Product Data Sheets. Elgin, Ill.: DSM Somos.

[10] "Accura™ Bluestone Nano-Composite Data Sheet." Valencia, Calif.: 3D Systems, March 2005.

[11] Viper SI2™ SLA® System Data Sheet. Valencia, Calif.: 3D Systems, March 2003.

[12] SLA® 7000 Data Sheet, Valencia, Calif.: 3D Systems, Feb. 2004.

[13] Jacobs, P.F. "Recent advances in rapid tooling from stereolithography." *Proc.* of 2nd Nat'l Conf. on RP and Tooling Research, Buckinghamshire College, 1996.